Effect of Temperature on the Corrosion Inhibition of Nonionic Surfactant TRITON-X-405 on Ferritic Stainless Steel in 1.0 M H2SO4

ARTICLE *in* INDUSTRIAL & ENGINEERING CHEMISTRY RESEARCH · JANUARY 2012

Impact Factor: 2.59 · DOI: 10.1021/ie2015697

3 AUTHORS, INCLUDING:

Regina fuchs-godec
University of Maribor
16 PUBLICATIONS **276** CITATIONS

SEE PROFILE

I&EC research
Industrial & Engineering Chemistry Research

ARTICLE

pubs.acs.org/IECR

Effect of Temperature on the Corrosion Inhibition of Nonionic Surfactant TRITON-X-405 on Ferritic Stainless Steel in 1.0 M H_2SO_4

Regina Fuchs−Godec,*[,†] Miomir G. Pavlović,[‡] and Milorad V. Tomić[‡]

[†]Faculty of Chemistry and Chemical Engineering, University of Maribor, Slovenia

[‡]Faculty of Technology Zvornik, University of Eastern Sarajevo, Republic of Srpska

ABSTRACT: The inhibiting action of a nonionic surfactant of the TRITON-X series (TRITON-X-405) on stainless steel type X4Cr13 in 1.0 M H_2SO_4 solution within the temperature range of 25−45 °C was studied using the gravimetric and potentiodynamic technique. The inhibition efficiency was found to increase with the inhibitor concentration and decrease with temperature. The satisfactory inhibition efficiency of TRITON-X-405 on SS type X4Cr13 in 1.0 M H_2SO_4 was limited to temperatures below 35 °C or at the surfactant concentration higher than $c = 10^{-5}$ M. The adsorption of TRITON-X-405 on stainless steel type X4Cr13 in one molar of sulphuric acid within the chosen temperature range follows the Flory−Huggins adsorption model with very high negative values of the free energy of adsorption ΔG_{ads}. The thermodynamic parameters, such as the heat of adsorption and adsorption entropy, were calculated by employing thermodynamic equations. Activation parameters such as apparent activation energy, activation enthalpy, and activation entropy were evaluated from the effect of temperature on corrosion and inhibition processes. Those entire apparent activation parameters show an increase−decrease characteristic (a nonmonotonic function). They increased at concentrations lower than the cmc of added surfactant and decreased when the concentration of TRITON-X-405 was higher than $c = 10^{-5}$ M.

1. INTRODUCTION

It is well-known that the corrosion of metallic structures has a significant impact on an economy, including infrastructure, transportation, utilities, production and manufacturing, and government. This is valid for any country of the developed world.[1] In regard to corrosion protection, various types of organic inhibitors have long been used during acid pickling, industrial acid cleaning, and acid descaling to control the acid corrosion of metals. Attempts have been made to study the corrosion of various types of steels and their inhibitions, by using different types of organic inhibitors in acid solution at higher temperatures.[2−9]

Surfactants represent a special and important category of organic inhibitors for the corrosion protection of metals in different corroding media, because of their dual affinity. When surfactants are used as inhibitors, they act through a process of surface adsorption. The hydrophilic parts of the molecules exhibit a very strong tendency to migrate to the surface and then adsorb, while the hydrophobic parts through the hydrophobic effect prevent the access of water molecules to the metal's surface. Inhibition is, however, maintained, on the basis of both effects. The extent of inhibition efficiency depends on the nature of the surfactant (ionic or nonionic types of surfactant, functional groups, critical micelle concentration cmc, etc.), the nature of the surface, and the corrosion medium (acid, base, temperature).[10−17]

Temperature has a very significant effect on the rate of metal corrosion. The increasing temperature is also responsible for any improvement or worsening of the surfactant's inhibition efficiency. Therefore, selecting an appropriate inhibitor for a specific environment and metal must be done with great care: it is known that an inhibitor that protects one particular metal may accelerate the corrosion of another.

They have been used as corrosion inhibitors of various materials such as steel,[16−25] copper,[15,26−32] brass,[33−37] and aluminum,[38−41] in different acidic solution, especially in HCl and H_2SO_4 at higher concentrations.

Nonionic surfactants represent a group, which is characterized by a much lower value of cmc as compared to ionic surfactants. This phenomenon can easily be explained by the fact that the free energy needed for bringing the polar heads together is much smaller when the headgroup is uncharged, than when it is charged. From this reason, the driving force of micellization is the hydrophobic force and van der Waal's attractions. A lower value of cmc is also an economic advantage, if the inhibiting efficiency is still sufficiently high at low concentrations of added surfactant ($c = 10^{-6}$ or 10^{-5} M).

Part of the presented study was actually an extension of our previous work[22,24] in which we investigated the inhibition abilities of two nonionic surfactants from the TRITON-X series. The objective of the presented work was to study the applicability of the nonionic surfactant TRITON-X-405 as a corrosion inhibitor for stainless-steel (SS) (type X4Cr13) in aqueous solutions of 1.0 M H_2SO_4 at higher temperatures. On the basis of classical thermodynamic data, such as adsorption heat, adsorption entropy, and adsorption free energy, an attempt was made to explain the adsorption phenomena of the chosen nonionic surfactant TRITON-X-405. These parameters were obtained from experimental data taken at several temperatures both in the presence and in the absence of the inhibitor.

Received: July 20, 2011
Accepted: December 3, 2011
Revised: December 1, 2011
Published: December 04, 2011

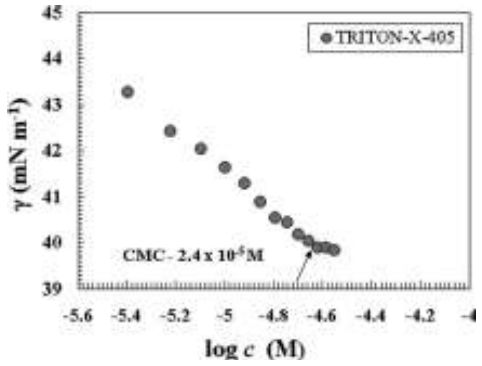

Figure 1. Variations of surface tension with concentration for TRITON-X-405, in 1.0 M H_2SO_4 at 25 °C.

2. MATERIALS AND METHODS

2.1. Materials. The nonionic surfactant used in the presented study was of the ethoxylated octyl phenyl alcohol type (Triton-X series, Fluka products), known as TRITON-X-405, with the following chemical structure and HLB value of 17.9 (HLB — hydrophile—lipophile balance values range from "0, completely lipophilic or oil-loving" to "20, completely hydrophilic or water-loving" and are calculated by dividing the weight percent of ethylene in the surfactant by 5, this valid only for nonionic surfactants).

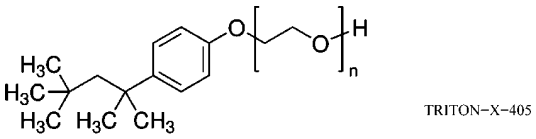

TRITON−X−405

n=40

$C_{14}H_{22}O{\cdot}(C_2H_4O)_n$

The inhibitor's concentration during the electrochemical study was within the range romf 1.0×10^{-6} to 1.0×10^{-4} M for TRITON-X-405. The aggressive solutions, 1.0 M H_2SO_4, were prepared by the dilution of AR grade 96% H_2SO_4 in distilled water. All of the solutions were prepared using water obtained from a Millipore Super-Q system. Electrochemical tests were performed on ferritic stainless steel of type X4Cr13, having composition in w %: C, 0.04; S, 0.02; Si, 0.471; Cr, 13.2; Ni, 0.307; Cu, 0.213; and balance Fe.

2.2. Surface Tension Measurements. The surface tension (γ) in 1.0 M H_2SO_4 was measured by the Wilhelmy-plate method, using a Krüss-K12 processor tensiometer, at a temperature of 25 °C. The temperature (±0.1 °C) was kept constant by circulating the thermostat-controlled water through a jacketed vessel containing the solution. The concentration of the solution varied by adding aliquots of stock solutions with known concentrations to the known volume of the solution in the vessel. The plate was cleaned over a flame (methane—butane).

The measured values for the surface tension were plotted as a function of the surfactant concentration logarithm, and the critical micelle concentration (cmc) was estimated from the break-point on the resulting curve. The representative plot of surface tension γ versus the logarithm at base 10 of the surfactant concentration $\log_{10} c$ is shown in Figure 1. The reproducibility of the surface tension versus concentration curve was checked by performing at least three separate experiments. The critical micelle concentration of the nonionic surfactant was determined to be $(2.4 \pm 0.2) \times 10^{-5}$ M for TRITON-X-405.

2.3. Weight Loss Experiment. Cylindrically shaped specimens of SS type X4Cr13 with a diameter of 16 mm and a thickness of 10 mm (and of 7—8 g average weight) were accurately weighted and then immersed in a 250 mL beaker for up to 2 h in a solution containing 1.0 M H_2SO_4 with and without addition of the TRITON-X-405 at 25.0, 30.0, 35.0, 40.0, and 45.0 °C, respectively. The temperature was controlled by an aqueous thermostat. All tests were made in the aerated solutions and were run in triplicate. All of the aggressive acid solutions were open to air. After 2 h, the specimens were taken out, washed, dried, and weighed accurately. The weight loss data were obtained from the average value of three parallel samples in 1.0 M H_2SO_4 with inhibitor at different concentrations.

2.4. Potentiodynamic Measurement. Polarization experiments were carried out using a conventional triple-electrode cell assembly with a platinum counter electrode (CE) and a saturated calomel electrode (SCE) coupled to a fine Luggin capillary as the reference electrode. The working electrode was of ferritic stainless steel type X4Cr13. The cylindrically shaped test specimens were fixed in a PTFE holder, and the geometric area of the electrode exposed to the electrolyte was 0.785 cm^2. During all experiments, electrochemical polarization was started 30 min after the working electrode was immersed in the solution, to allow for stabilization of the stationary potential.[15−17] Before each measurement, the sample was cathodically polarized at −1.0 V (SCE) for 10 min and then allowed to reach a stable open-circuit potential, which was attained after about 30 min. The potentiodynamic current potential curves were recorded by automatically changing the electrode potential from −0.7 to 0.9 V (SCE) at a scanning rate of 2 mV s^{-1}. All of the experiments were performed within a range of temperature from 25 to 45 °C in both the presence and the absence of an inhibitor. A SOLATRON 1287 Electrochemical Interface was used to apply and control the potential. The data were collected using CorrWare and interpreted with CorrView software. All of the software was developed by Scribner Associates, Inc. The metal surface was hand-polished successively using emery papers of grade 400, 600, 800, 1000, and 1200. Finally, the specimen was fine polished with diamond paste to obtain a shiny and clear surface, like a mirror. After being polished, the working electrode was washed with water and degreased using acetone.

3. RESULTS AND DISCUSSION

3.1. Electrochemical Results. Figure 2 shows the potentiodynamic polarization curves for ferritic stainless steel type X4Cr13 in 1.0 M H_2SO_4 solution containing various concentrations of TRITON-X-405 at five different temperatures (in the range of 25—45 °C). In all cases, the presence of TRITON-X-405 caused a remarkable decrease in the anodic and cathodic currents' densities and a shifting of the anodic curves to positive potentials (Figure 3). This may be ascribed to the adsorption of the inhibitor over the corroded surface. Following a rise in the temperature, this phenomenon became less-noticeable, especially at those concentrations that were lower than cmc. An interesting phenomenon occurred at 25 °C, when any further increase in the concentration of TRITON-X-405 (up to 3 orders of magnitude) had no appreciable influence on increasing the

dx.doi.org/10.1021/ie2015697 |Ind. Eng. Chem. Res. 2012, 51, 274–284

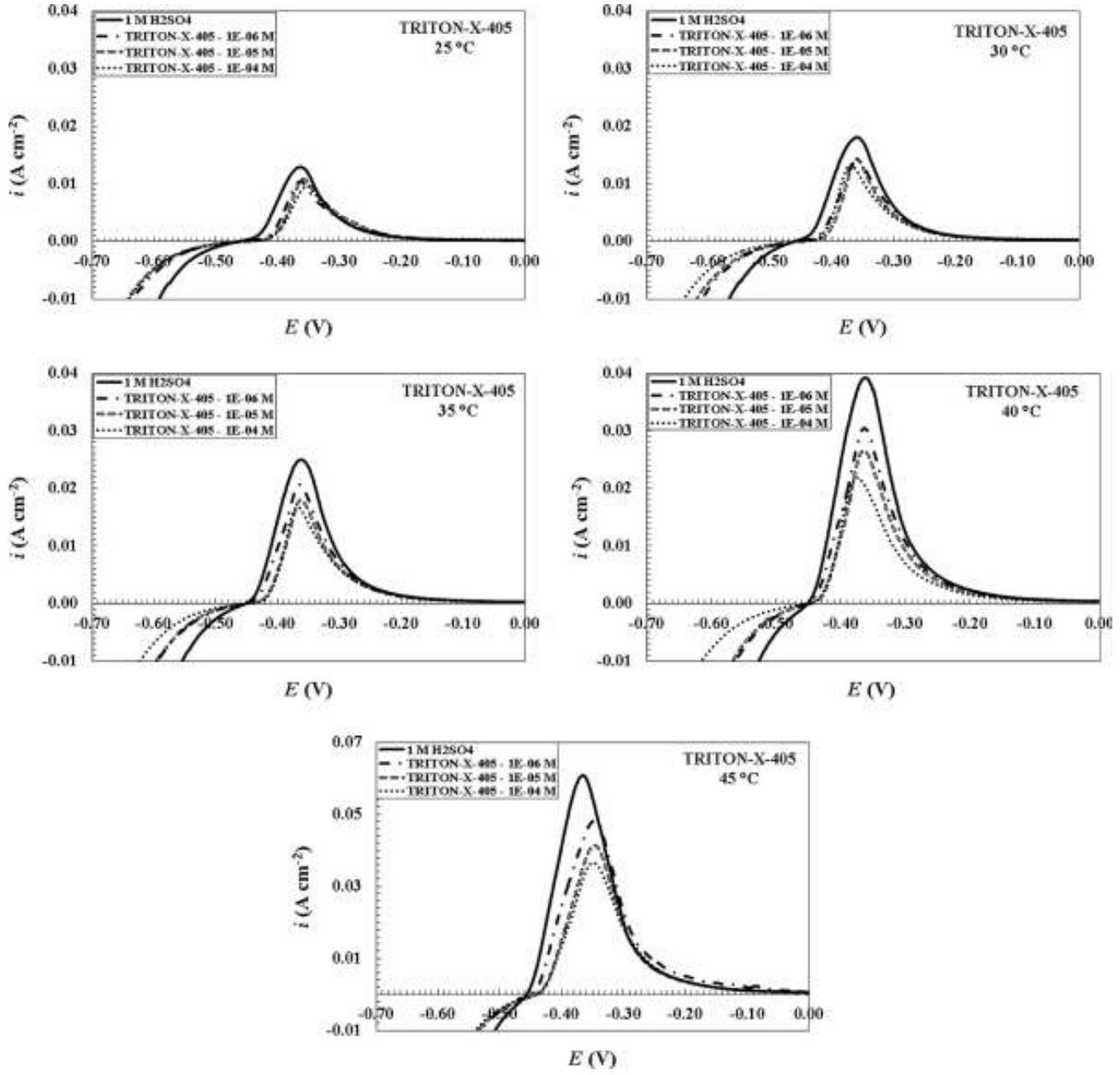

Figure 2. Temperature dependence of the anodic polarization curves of stainless steel type X4Cr13 in a mixture of 1.0 M H_2SO_4 containing various concentrations of TRITON-X-405. All of the potentials were measured against the saturated calomel electrode (SCE).

inhibition's efficiency. This occurrence slowly disappeared with increasing temperature.

The electrochemical parameters (as obtained from polarization curves) including corrosion current densities (i_{corr}), corrosion potential (E_{corr}), polarization resistance (R_p), and surface coverage θ are listed in Table 1.

The polarization resistance was calculated by taking the slope of the nonlinear part of the Tafel plot, where linear polarization techniques curve within the potential range of ± 10 mV with respect to E_{corr}. Extrapolation of the Tafel line (i.e., linear part of the Tafel plots) to the free corrosion-potential allowed us to calculate the corrosion current density $i_{corr.}$ All of the parameters were determined simultaneously by CorrView software, which was provided with a SOLATRON 1287 potentiostat.

3.2. Adsorption Isotherms. The corrosion inhibition process is based on an adsorption of the inhibitor's molecules on the metal's surface. Therefore, it is of great importance to find an appropriate adsorption isotherm that fits the experimental results. It is well-known that adsorption isotherms provide useful insights into the mechanism of corrosion inhibition. The values for surface coverage θ for various concentrations of the used inhibitor under this investigation were calculated via those electrochemical parameters measured during the corrosion processes, as well as the polarization resistance R_p, and the corrosion current density i_{corr}, using the following equations:

$$\theta = 1 - \frac{i'_{corr}}{i_{corr}} \quad (1)$$

dx.doi.org/10.1021/ie2015697 |Ind. Eng. Chem. Res. 2012, 51, 274–284

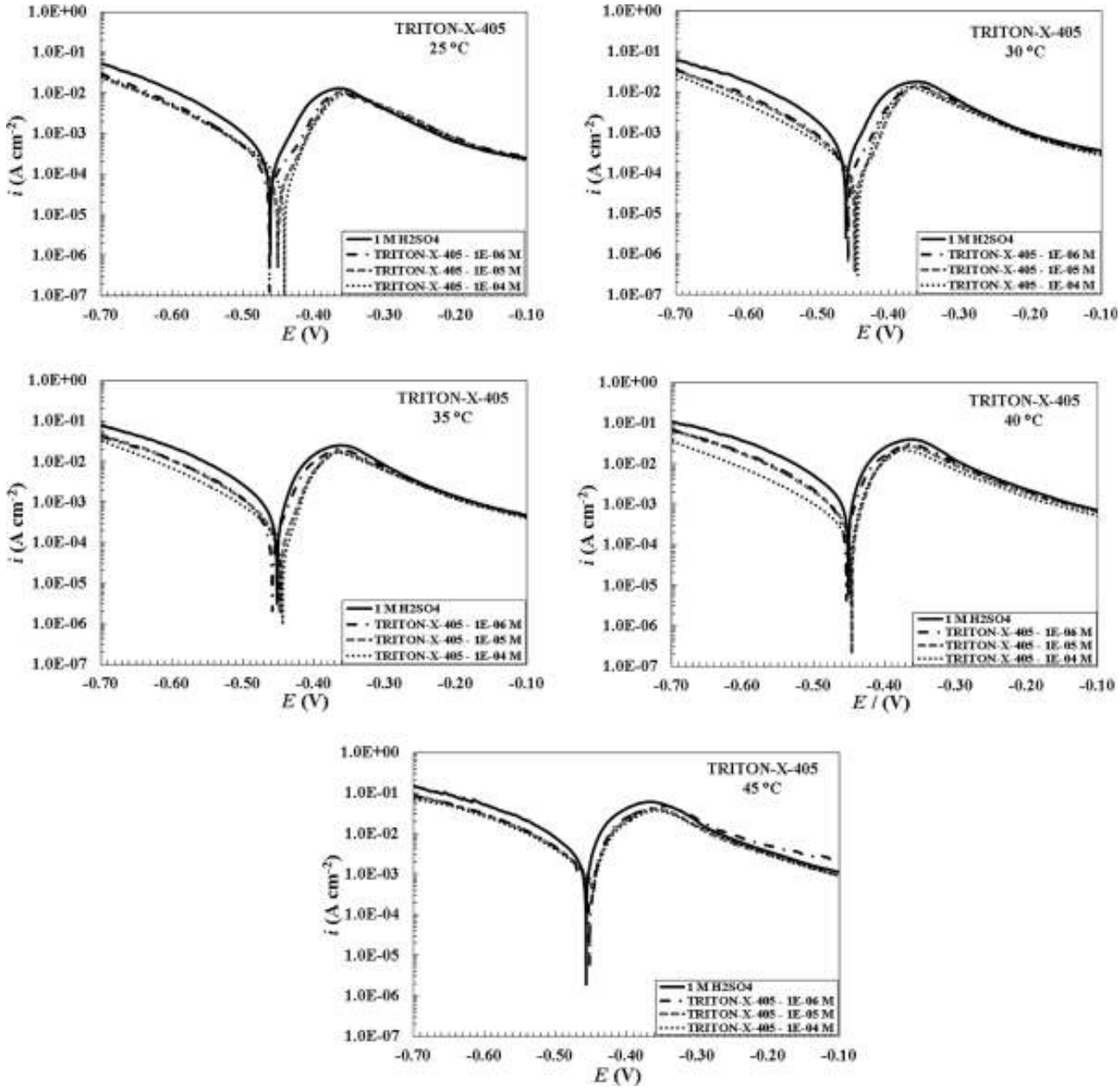

Figure 3. Influence of added TRITON-X-405 on the cathodic and anodic behavior of stainless steel X4Cr13 in 1.0 M H_2SO_4 at different temperatures. All of the potentials were measured against the saturated calomel electrode (SCE).

$$\theta = 1 - \frac{R_p}{R_p'} \tag{2}$$

The notation i_{corr} and R_p were used for those measurements without added surfactant, while the primed quantities i_{corr}' and R_p' applied when surfactant was added to a solution of 1.0 M H_2SO_4. Attempts were made to fit θ values to standard isotherms including that of Frumkin, Flory–Huggins, Langmuir, Bockris–Swinkels, and Temkin. By far, the best fit was obtained by assuming the Flory–Huggins in the form given by eq 3:

$$\log\left[\frac{\theta}{c_{inh}}\right] = \log(xK_{ads}) + x\log[1-\theta] \tag{3}$$

The calculated values for the surface coverage θ for TRITON-X-405 in 1.0 M H_2SO_4 are also reported in Table 1.

According to the Flory–Huggins model, plots of $\log[\theta/c]$ versus $\log[1-\theta]$ give straight lines with a slope x and an intercept $\log(xK_{ads})$ as shown in Figure 4. The plot indicates that the values of x changed from 18.3 to 6.2 with increasing temperature. This suggests that one molecule of adsorbed TRITON-X-405 on the metal's surface replaced more than 18 water molecules at 25 °C and reduced to around 6 at 45 °C. (The same behavior was obtained in the case where θ was evaluated from the polarization resistance.)

As mentioned previously, the TRITON-X-405 had difficulty when organizing and packing onto the metal's surface, probably because of its size. In our previous studies, it was confirmed that

dx.doi.org/10.1021/ie2015697 |Ind. Eng. Chem. Res. 2012, 51, 274–284

Table 1. Electrochemical Parameters for the Corrosion of SS Type X4Cr13, As Obtained from Potentiodynamic Polarization Curves and Corrosion Rate Obtained from the Weight Loss Test at Various Temperatures in 1.0 M H_2SO_4, Containing Various Concentrations of TRITON-X-405

1.0 M H_2SO_4 + x M TRITON-X-405	i_{corr} (A cm^{-2})	E_{corr} (V vs SCE)	R_p (Ω cm^{-2})	$\theta_{i_{corr}}$	θ_{R_p}	W (mg cm^{-2} h^{-1})	θ_W
		25 °C					
0	3.92×10^{-4}	−0.463	41.08			0.410	
1.0×10^{-6}	1.33×10^{-4}	−0.460	124.24	0.661	0.669	0.144	0.650
5.0×10^{-6}	1.19×10^{-4}	−0.457	135.60	0.696	0.697	0.128	0.688
1.0×10^{-5}	1.13×10^{-4}	−0.436	142.13	0.712	0.711	0.123	0.700
5.0×10^{-5}	1.07×10^{-4}	−0.431	150.43	0.727	0.727	0.115	0.719
1.0×10^{-4}	1.04×10^{-4}	−0.425	158.20	0.734	0.740	0.111	0.729
		30 °C					
0	7.21×10^{-4}	−0.462	28.23			0.755	
1.0×10^{-6}	2.79×10^{-4}	−0.456	73.48	0.612	0.615	0.294	0.609
5.0×10^{-6}	2.22×10^{-4}	−0.453	84.24	0.692	0.665	0.237	0.685
1.0×10^{-5}	2.11×10^{-4}	−0.446	94.13	0.707	0.701	0.233	0.691
5.0×10^{-5}	1.95×10^{-4}	−0.445	99.74	0.729	0.717	0.215	0.715
1.0×10^{-4}	1.93×10^{-4}	−0.443	107.18	0.732	0.736	0.205	0.728
		35 °C					
0	9.49×10^{-4}	−0.460	19.13			0.995	
1.0×10^{-6}	3.98×10^{-4}	−0.458	45.18	0.580	0.576	0.388	0.577
5.0×10^{-6}	3.67×10^{-4}	−0.455	55.63	0.613	0.656	0.312	0.608
1.0×10^{-5}	3.04×10^{-4}	−0.447	59.78	0.679	0.680	0.307	0.669
5.0×10^{-5}	2.67×10^{-4}	−0.446	68.46	0.718	0.720	0.283	0.701
1.0×10^{-4}	2.56×10^{-4}	−0.446	71.11	0.730	0.731	0.270	0.725
		40 °C					
0	1.68×10^{-3}	−0.460	11.171			1.765	
1.0×10^{-6}	7.33×10^{-4}	−0.454	22.48	0.563	0.503	0.777	0.557
5.0×10^{-6}	7.22×10^{-4}	−0.448	28.01	0.570	0.601	0.762	0.566
1.0×10^{-5}	5.86×10^{-4}	−0.446	32.18	0.652	0.653	0.625	0.644
5.0×10^{-5}	4.95×10^{-4}	−0.442	37.90	0.705	0.705	0.532	0.697
1.0×10^{-4}	4.54×10^{-4}	−0.448	41.34	0.729	0.730	0.532	0.717
		45 °C					
0	2.87×10^{-3}	−0.459	4.799			3.010	
1.0×10^{-6}	1.59×10^{-3}	−0.466	8.355	0.444	0.425	1.692	0.438
5.0×10^{-6}	1.39×10^{-3}	−0.464	10.771	0.516	0.554	1.499	0.502
1.0×10^{-5}	1.23×10^{-3}	−0.439	11.893	0.570	0.596	1.327	0.559
5.0×10^{-5}	9.32×10^{-4}	−0.446	14.907	0.675	0.678	1.002	0.667
1.0×10^{-4}	8.52×10^{-4}	−0.441	16.490	0.703	0.709	0.936	0.689

desorption of the protective layer formed in the presence of TRITON-X-405 starts sooner, as in the case of TRITON-X-100.[22] The free species, which appear on the metal surface between monomers or micelles, also represent those active points that initialize the corrosion process. With increasing temperature, the mobility of surfactant molecules also increases. This phenomenon additionally impedes the adsorption of the surfactant molecules on the metal's surface. This could be just one possible explanation as to why adsorption becomes unfavorable with increasing temperature. Figure 5 represents the corrosion inhibition efficiency (IE = $\theta \times 100$) for TRITON-X-405 on SS type X4Cr13 in 1.0 M H_2SO_4 as a function of temperature and the concentration of added nonionic surfactant. The good inhibition efficiency of TRITON-X-405 for the chosen system was limited to temperatures below 35 °C or for the surfactant concentration higher than $c = 10^{-5}$ M, as it is shown in Figure 5.

3.3. Thermodynamic Parameters. The free energy of adsorption ΔG_{ads} is an important thermodynamic parameter, because it provides useful information about the type of adsorption process. In general, values for the free energy of adsorption ΔG_{ads}, up to −20 kJ mol^{-1}, seem to suggest electrostatic interaction between the charged molecules and the charged metal (physical adsorption), while those more negative than −40 kJ mol^{-1} involve charge sharing or transfer from the inhibitor's molecules to the metal surface, to form a coordinate type of bond (chemisorption).

Equation 4 represents the relationship between the free energy of adsorption ΔG_{ads} and the modified adsorption equilibrium constant K_{ads}. Further, $c_{solvent}$ is the molar concentration of

dx.doi.org/10.1021/ie2015697 |Ind. Eng. Chem. Res. 2012, 51, 274–284

solvent, which, in the case of water, is 55.5 mol L^{-1}.

$$K_{ads} = \frac{1}{c_{solvent}} \exp\left(\frac{-\Delta G_{ads}}{RT}\right) \quad (4)$$

The ΔG_{ads} values were calculated from eq 4. They are negative and in accordance with eq 4, suggesting the spontaneity of the adsorption process. Furthermore, the calculated values of ΔG_{ads} for TRITON-X-405 are within the range from −85.0 to approximately −49.0 kJ mol^{-1}, so chemisorption is supposed (Table 2). This finding seems to be consistent with the molecular structure of this particular surfactant, the structure of which allows for adsorption on the metal's surface via two lone-pairs of electrons on the oxygen atoms.

ΔG_{ads} increased with increasing temperature (Figure 6). This phenomenon, in accordance with previous explanations, confirms our prediction that the adsorption becomes unfavorable with increasing temperature, as the result of a desorption of the inhibitor from the steel surface. When the temperature is higher than 35 °C, the adsorbed inhibitors tend toward desorption, especially at a concentration that is lower than the cmc of the TRITON-X-405. It seems that this phenomenon could be confirmed by the electron microscope images, as shown in Figure 7. The image of the surface exposed to the chosen solution (Figure 7b) at higher temperatures shows much more of a heterogeneous layer of corrosion and just single parts or spots where TRITON-X-405 could be adsorbed on the metal's surface, in comparison with the covered parts visible in Figure 7a. On the other hand, when the temperature increased, the corrosion rate also becomes higher, and the destructive effect of the anodic process on the self-assembling layer becomes predominant. Such behavior likewise reduces the possibility of adsorption by the organic molecules on the metal's surface. Reduction of the adsorption equilibrium constant K_{ads} with temperature also indicates that nonionic surfactant TRITON-X-405 is easily adsorbed onto the steel surface at lower temperatures.

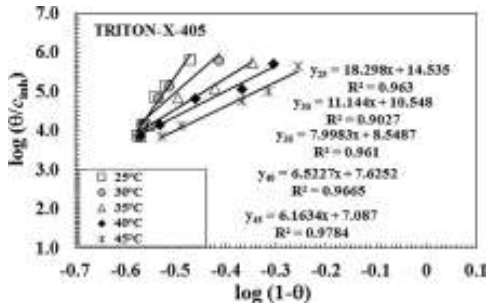

Figure 4. Flory−Huggins adsorption isotherm for TRITON-X-405 on SS type X4Cr13 in 1.0 M H_2SO_4 at different temperatures; θ is obtained from the corrosion current density (i_{corr}).

Thermodynamic parameters, including the adsorption heat ΔH_{ads} and the standard adsorption entropy ΔS_{ads}, were calculated using the following equations; under the experimental conditions, the adsorption heat could be approximately regarded as the standard adsorption heat and could be calculated according to the van't Hoff equation as given by eq 5:

$$\ln K_{ads} = -\frac{\Delta H_{ads}}{RT} + \text{const} \quad (5)$$

The standard adsorption entropy ΔS_{ads} was calculated according to the thermodynamic basic equation (eq 6).

$$\Delta G_{ads} = \Delta H_{ads} - T\Delta S_{ads} \quad (6)$$

Figure 8 shows the plot of ln K_{ads} versus $1/T$, which gives a straight line with a slope of $(-\Delta H_{ads}/R)$ and intercept $(-\Delta S_{ads}/R - \ln 55.5)$. The ΔH_{ads} value calculated from eq 5 is −604.72 kJ mol^{-1}. The negative sign of ΔH_{ads} indicates that the adsorption of the chosen nonionic surfactants on the steel surface in 1.0 M H_2SO_4 solution is an exothermic process. A more negative value for ΔH_{ads} was obtained in comparison with nonionic surfactant TRITON-X-100 (−320.41 kJ mol^{-1}).[24] This indicates a greater ability toward inhibition. Knowing ΔG_{ads} and ΔH_{ads}, we can now calculate ΔS_{ads}. All of the obtained thermodynamic parameters are collected in Table 2.

The calculated values for ΔS_{ads} are negative and indicate that the process of adsorption is accompanied by a decrease in entropy. The obtained value for the standard adsorption entropy ΔS_{ads} was twice as much and more negative than in the case of TRITON-X-100.[24] We may assume that before the adsorption, inhibitor molecules freely moved in solution. A molecule of TRITON-X-405 is much bigger than that of TRITON-X-100 (TRITON-X-100 contains 9−10 ethylene oxide groups and TRITON-X-405 around 40 ethylene oxide groups). From this reason, the entropy of the system was higher in the case of

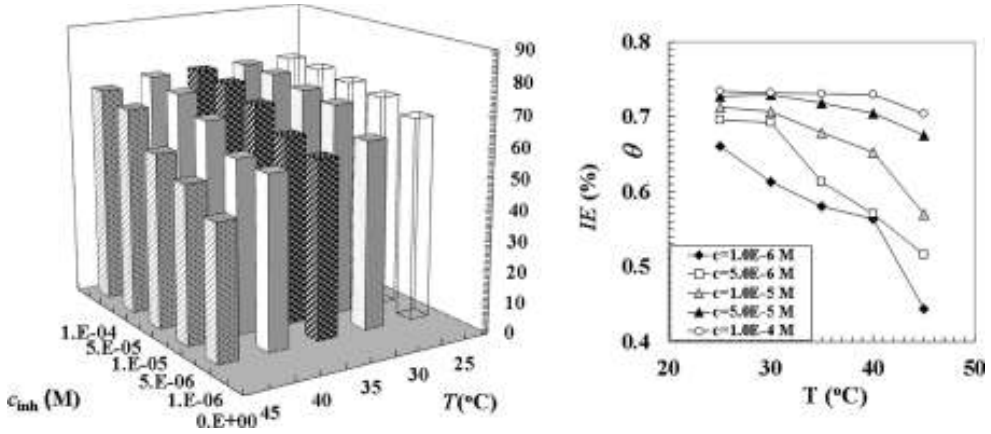

Figure 5. The corrosion inhibition efficiency (IE = $\theta \times 100$) for TRITON-X-405 of SS type X4Cr13 in 1.0 M H_2SO_4 (obtained from i_{corr}) investigated in the range of temperatures from 25 to 45 °C.

Table 2. Thermodynamic Parameters for Adsorption of the TRITON-X-405 on the Surface of SS Type X4Cr13 in 1.0 M H_2SO_4, at Different Temperatures

T (K)	K_{ads} (M^{-1})	ΔG_{ads} (kJ mol^{-1})	ΔH_{ads} (kJ mol^{-1})	ΔS_{ads} (J mol^{-1} K^{-1})
298.15	1.87×10^{13}	−85.71		−1740.76
303.15	3.17×10^{9}	−65.26		−1779.51
308.15	4.42×10^{7}	−55.39	−604.72	−1782.66
313.15	6.47×10^{6}	−51.29		−1767.31
318.15	2.25×10^{6}	−48.98		−1746.79

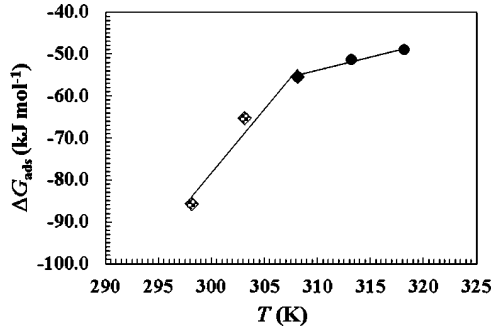

Figure 6. The free energy of adsorption ΔG_{ads} for TRITON-X-405 in 1.0 M H_2SO_4 investigated within a range of temperatures from 25 to 45 °C.

TRITON-X-405. Through the adsorption process, the inhibitor's molecules were orderly adsorbed onto the metal surface. A decrease in entropy could be an adequate explanation for a phenomenon such as this.

3.4. Weight Loss Measurements, Adsorption Isotherm, and Thermodynamic Parameters. Weight loss data, that is, the mean corrosion rate W and the surface coverage values θ of X4Cr13 SS in 1.0 M H_2SO_4 in the absence and presence of various concentrations of TRITON-X-405, were obtained and are given in Table 1. Figure 9 represents the mean corrosion rate W of the SS type X4Cr13 as function of temperature and concentration of added nonionic surfactant TRITON-X-405 in 1.0 M H_2SO_4. It was calculated on the basis of the weight loss experiment, expressed as in mg cm^{-2} h^{-1}. As the temperature of the inhibitor's free solution increases above the 35 °C, the corrosion rate increases progressively. Moreover, the good inhibition properties of TRITON-X-405 on SS type X4Cr13 in 1.0 M H_2SO_4 were limited again to temperatures below 35 °C or for the surfactant concentration higher than $c = 10^{-5}$ M, as it was shown in Figure 5 already. The effects shown in Figure 9 are in good accordance with results that were obtained from potentiodynamic measurements. The degree of surface coverage θ was calculated according to eq 7:

$$\theta = 1 - \frac{W}{W'} \tag{7}$$

where W and W' are the mean corrosion rate of X4Cr13 SS in the absence and presence of the nonionic surfactant TRITON-X-405, respectively. The surface coverage values were also tested graphically for fitting a suitable adsorption isotherm. The same behavior and agreement with the Flory−Huggins adsorption isotherm were obtained with a little difference in the slope (x)

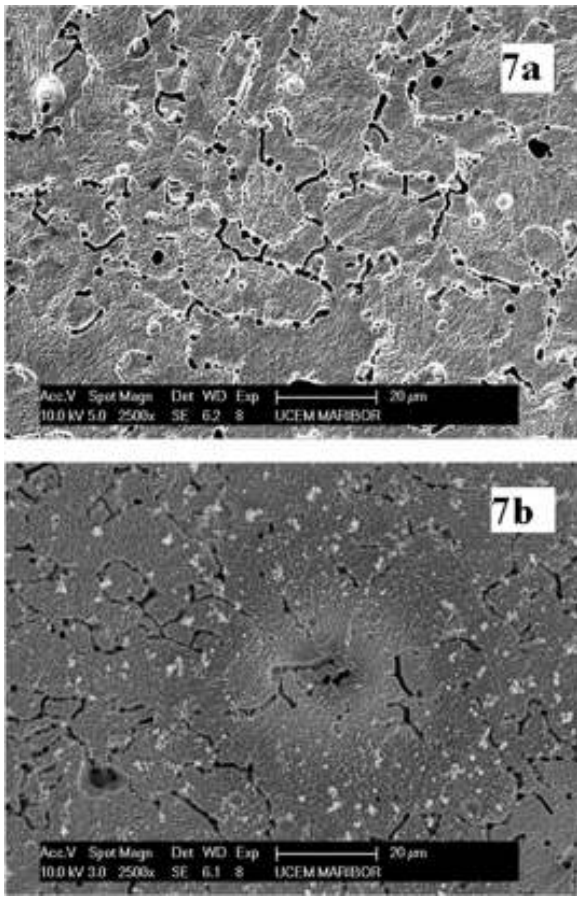

Figure 7. SEM pictures of an X4Cr13 SS electrode's surface: (a) with 1×10^{-5} M added TRITON-X-405 at 25 °C, and (b) with 1×10^{-5} M added TRITON-X-405 at 40 °C in 1.0 M H_2SO_4.

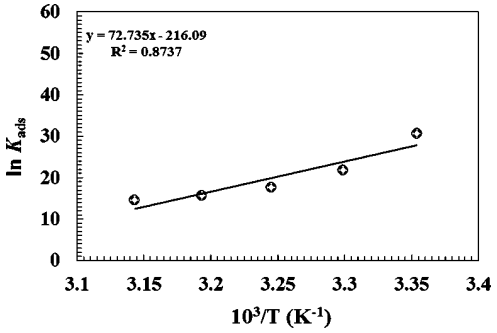

Figure 8. The relationship between ln K_{ads} and the reciprocal value of the absolute temperature T^{-1}.

and intercept $\log(xK)$ as shown in Figure 10. Therefore, some differences are also obtained for the ΔG_{ads} and for the adsorption equilibrium constant K_{ads} (Table 3).

The values of the free energy of adsorption are a little more negative, while the values of the adsorption equilibrium constant are higher with respect to those obtained from the polarization measurement. The possible answer could be found in the fact that the polarization method is faster than gravimetric and the corrosion inhibitors act by different mechanisms (anodic, cathodic, or mixed type), and some may act faster than others. Corrosion reactions are

dx.doi.org/10.1021/ie2015697 |*Ind. Eng. Chem. Res.* 2012, 51, 274–284

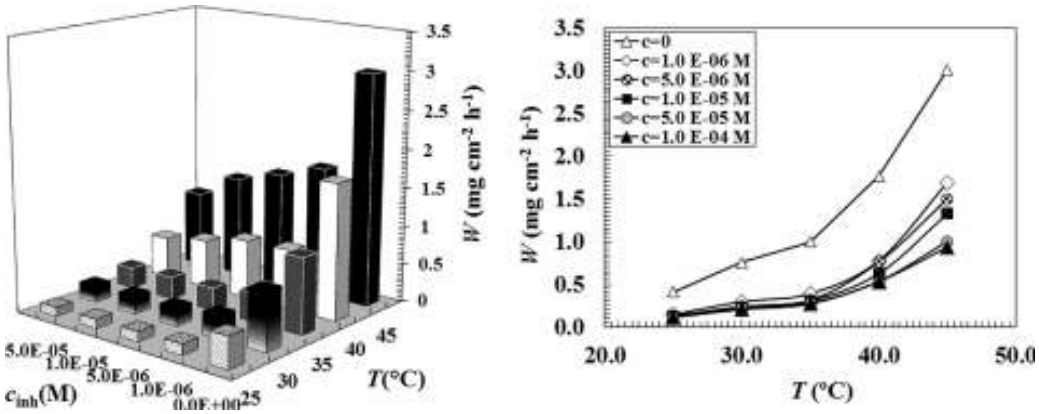

Figure 9. The mean corrosion rate W of the SS type X4Cr13 as a function of temperature and concentration of added nonionic surfactant TRITON-X-405 in 1.0 M H_2SO_4.

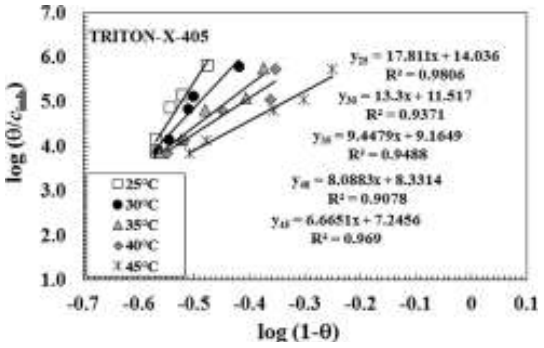

Figure 10. Flory−Huggins adsorption isotherm for TRITON-X-405 on SS type X4Cr13 in 1.0 M H_2SO_4 at different temperatures; θ is obtained from the mean corrosion rate W (weight loss test).

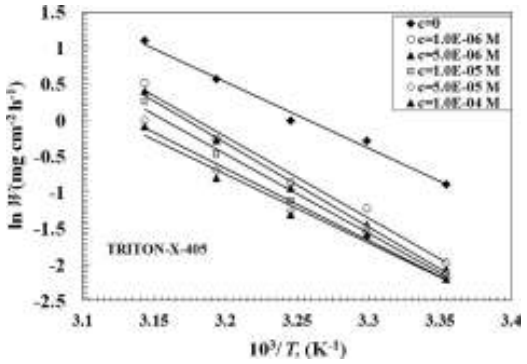

Figure 11. Eyring transition stat plots for TRITON-X-405 of SS type X4Cr13 in 1.0 M H_2SO_4 at different temperatures (T is absolute temperature).

Table 3. Adsorption Parameters K_{ads} and ΔG_{ads} Calculated from the Data of the Weight Loss Measurement

T (°C)	K_{ads}	ΔG_{ads} (kJ mol^{-1})
25	6.10×10^{12}	−82.93
30	$2.47 \times 10^{1}0$	−70.44
35	1.55×10^{8}	−58.60
40	2.65×10^{7}	−54.96
45	2.64×10^{6}	−49.74

usually regarded as Arrhenius processes.[42−46] Corrosion rate increases exponentially with temperature because the hydrogen evolution overpotential decreases; therefore, the dependence of a corrosion rate W on temperature can be expressed by the Arrhenius equation given by eq 8:

$$W = A \exp\left(\frac{-E_a}{RT}\right) \quad (8)$$

where E_a represents the apparent activation energy, R is the general gas constant, T is the absolute temperature, A is the Arrhenius pre-exponential constant depending on the metal type and the electrolyte, and W is the corrosion rate obtained from the weight loss method. The activation energy can be calculated from the slope, by plotting the natural logarithm of the corrosion rate against $1/T$. Arrhenius plots for the corrosion rate of SS type X4Cr13 in 1.0 M H_2SO_4 + x M TRITON-X-405 at different temperatures are given in Figure 11. The negative slope of E_a indicates the adsorption of organic compounds on the metal surface. The values of the apparent activation energies obtained for various concentrations of the TRITON-X-405 at 25−45 °C are given in Table 4. It is clear that the activation energies of the corrosion process for protecting steel using the tested inhibitor are higher than that of the unprotected SS in 1.0 M H_2SO_4 solution. The greater increase for the activation energy in the presence of the inhibitor indicates higher inhibition efficiency for the inhibitor regarding the chosen system. However, in the present study, it was found that with increasing concentrations of TRITON-X-405, the apparent activation energy first increased, and then decreased. Actually, it started to decrease when the concentrations of added nonionic surfactant became higher than the cmc value of the chosen nonionic surfactant (Figure 12). The variations in the pre-exponential factors showed the same characteristics as in the case of the apparent activation energy. It was reported that any increase of E_a in the presence of the inhibitor indicates physisorption or weak chemical bonding between the inhibitor molecules and the metal surface, and later decreases of the apparent activation energy at concentrations higher than added inhibitor lead to a change in the mechanism, to chemisorption.[42−46]

Mazhar[47] et al. explained that the increase in the activation energy with respect to uninhibited solutions could be related

Table 4. Activation Parameters and Arrhenius Parameter *A* of Dissolution Reaction of SS Type X4Cr13 in 1.0 M H_2SO_4 at Different Concentrations of Added TRITON-X-405

1.0 M H_2SO_4 + *x* M TRITON-X-405	Arrhen. parameter *A* (mg cm^{-2} h^{-1})	ΔE_a (kJ mol^{-1})	ΔH^* (kJ mol^{-1})	ΔS^* (J $mol^{-1}K^{-1}$)	linear correl. coeff.
0	9.37×10^{12}	76.23	73.49	62.30	0.988
1.0×10^{-6}	3.43×10^{15}	93.54	91.31	111.99	0.985
5.0×10^{-6}	9.74×10^{15}	96.49	92.33	120.67	0.995
1.0×10^{-5}	9.94×10^{14}	90.95	88.71	102.55	0.986
5.0×10^{-5}	2.81×10^{13}	82.25	79.69	73.20	0.983
1.0×10^{-4}	7.71×10^{12}	79.05	75.17	61.30	0.982

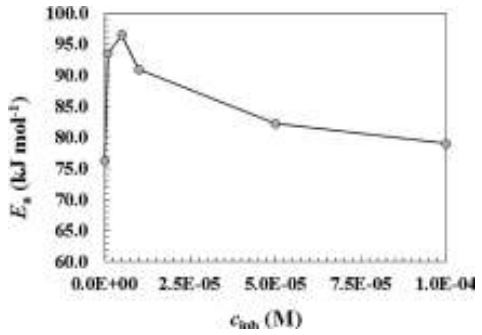

Figure 12. Dependence of the apparent activation energy on the concentrations of added TRITON-X-405.

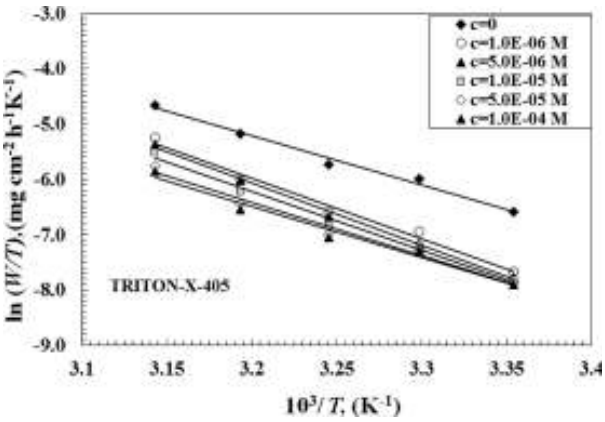

Figure 13. Eyring transition stat plots of $\ln(W/T)$ versus T^{-1} for SS type X4Cr13 in 1.0 M H_2SO_4 with TRITON-X-405 at different concentrations.

with diffusion processes, especially when values of activation energies are higher than 60.0 kJ mol^{-1}. This phenomenon could indicate that the diffusion of metal ions through the protective film on the metal surface is rate controlling. The higher values of E_a in the presence of the inhibitors as compared to the uninhibited solutions suggest that the presence of the inhibitor at the electrode/electrolyte interface leads to an increase in the energy barrier of the alloy dissolution. At c_{inh} > cmc, the micelles cover the entire surface quickly and, possibly at the same time, block access to the active site of corrosion on the surface, again reducing the chance of attack at these sites. Because of effective blocking (formation of a compact barrier film) of the whole exposed surface, the diffusion process is impeded or stopped. This could be a possible explanation for the decreasing of the activation energy with increasing concentration of added nonionic surfactant. It should be noted that they are still higher with respect to uninhibited solutions.

On the basis of the obtained values of E_a, the thermodynamic parameters of activation for the corrosion process were calculated. Thermodynamic parameters including enthalpy of activation ΔH^* and entropy of activation (ΔS^*) were calculated using the Eyring transition state equation (eq 9).[48,49]

$$W = \frac{RT}{N_A h} \exp\left(\frac{-S^*}{R}\right) \exp\left(-\frac{\Delta H^*}{RT}\right) \quad (9)$$

where N_A is the Avogadro number, h is Planck's constant, and other terms retain their previous meanings. Figure 13 show plots of $\ln(W/T)$ versus $1/T$ obtained in 1.0 M H_2SO_4 without and with the addition of the TRITON-X-405. The straight lines were obtained with a slope of $-\Delta H^*/R$ and intercept of $[\ln(R/N_A h) + \Delta S^*/R]$ from which the values of ΔH^* and ΔS^* were calculated and listed in Table 4.

The positive values of ΔH^* both in the absence and in the presence of inhibitor reflect the endothermic nature of the steel dissolution process. Also, the values of ΔS^* were higher for solutions where concentrations of added TRITON-X-405 are lower than the cmc. This could be explained by an increase of disorder in the vicinity and on the surface of the metal. The adsorption of the organic inhibitor was accompanied by desorption of water molecules from the surface. Actually, the activation enthalpies and entropies vary in the same manner as the activation energies, that is, increase with increasing concentrations of TRITON-X-405 until the cmc is exceeded, then begin to decrease. It could be speculated that through the adsorption process inhibitor molecules were orderly adsorbed onto the surface. A decrease in entropy could be a satisfactory answer (ΔS^*, positive; ΔS_{ads}, negative; this indicates the exchange from disorder to order).

4. CONCLUSIONS

Satisfactory inhibition efficiency for TRITON-X-405 of SS type X4Cr13 in 1.0 M H_2SO_4 was limited to temperatures below 35 °C or at surfactant concentrations higher than $c = 10^{-5}$ M.

The shift in rest potential E_{corr} toward a more noble value was only noticeable at 25 °C; with increasing temperature, this phenomenon disappeared again or is irrelevant.

The adsorption of nonionic surfactant TRITON-X-405 on stainless steel type X4Cr13 in one molar sulphuric acid in the range of temperatures 25−45 °C follows the Flory−Huggins adsorption model.

dx.doi.org/10.1021/ie2015697 |*Ind. Eng. Chem. Res.* 2012, 51, 274–284

The investigated inhibitor was also suggested to be chemisorbed on the electrode surface, on the basis of the high values for the adsorption equilibrium constant K_{ads} and the free energy of adsorption, ΔG_{ads}.

The thermodynamic values obtained from this study indicate exothermic and spontaneous behavior by the adsorption of TRITON-X-405 on the steel surface $\Delta H_{ads} < 0$.

Throughout the adsorption process, the inhibitor's molecules were orderly adsorbed onto the surface (formed a more organized structure), $\Delta S_{ads} < 0$.

The apparent activation energy E_a increased at concentrations lower than the cmc of the added surfactant and decreased when the concentration of TRITON-X-405 was higher than $c = 10^{-5}$ M. This could indicate that the diffusion of metal ions through the protective film on the metal surface is rate controlling when $c_{inh} <$ cmc.

AUTHOR INFORMATION

Corresponding Author

*E-mail: fuchs@uni-mb.si.

ACKNOWLEDGMENT

This work was financially supported by the Ministry of Science and Technology Republic of Srpska under the research project "Use of Surface Active Agents (Surfactants) in Sense the Protection of Construction Materials Against Corrosion" (no. 06/0-020/961-239/10) and by the Slovenian Research Agency under the reseach project "Physico-Chemical Processes on the Surface Layers and Application of Nanoparticles" (P2-0006).

REFERENCES

(1) Koch, G.; Brongers, M.; Thompson, N.; Virmani, Y.; Payer, J. Report # FHWA-RD-01-156,Corrosion Cost and Preventive Strategies in the United States; Office of Infrastructure Research and Development, Federal Highway Administration: McLean, VA, 2001.

(2) Popova, A.; Christov, M.; Vasilev, A. Inhibitive properties of quaternary ammonium bromides of N-containing heterocycles on acid mild steel corrosion. Part I: Gravimetric and voltammetric results. *Corros. Sci.* **2007**, *49*, 3276.

(3) Bentiss, F.; Bouanis, M.; Mernari, B.; Traisnel, M.; Vezin, H.; Lagrenée, M. Understanding the adsorption of 4*H*-1,2,4-triazole derivatives on mild steel surface in molar hydrochloric acid. *Appl. Surf. Sci.* **2007**, *253*, 3696.

(4) Qiu, L.; Wu, Y.; Wang, Y.; Jiang, X. Synergistic effect between cationic gemini surfactant and chloride ion for the corrosion inhibition of steel in sulphuric acid. *Corros. Sci.* **2008**, *50*, 576.

(5) Abboud, Y.; Abourriche, A.; Saffaj, T.; Berrada, M.; Charrouf, M.; Bennamara, A.; Cherqaoui, A.; Takky, D. The inhibition of mild steel corrosion in acidic medium by 2,2′-bis(benzimidazole). *Appl. Surf. Sci.* **2006**, *252*, 8178.

(6) Oguzie, E. E.; Njoku, V. O.; Enenebeaku, C. K.; Akalezi, C. O.; Obi, C. Effect of hexamethylpararosaniline chloride (crystal violet) on mild steel corrosion in acidic media. *Corros. Sci.* **2008**, *50*, 3480.

(7) Obot, I. B.; Obi-Egbedi, N. O. Adsorption properties and inhibition of mild steel corrosion in sulphuric acid solution by ketoconazole: Experimental and theoretical investigation. *Corros. Sci.* **2010**, *52*, 198.

(8) Popova, A. Temperature effect on mild steel corrosion in acid media in presence of azoles. *Corros. Sci.* **2007**, *49*, 2144.

(9) Li, X.; Deng, S.; Mu, G.; Fu, H.; Yang, F. Inhibition effect of nonionic surfactant on the corrosion of cold rolled steel in hydrochloric acid. *Corros. Sci.* **2008**, *50*, 420.

(10) Villamil, R. F. V.; Cordeiro, G. G.; Matos, J.; D'Elia, E.; Agostinho, S. M. L. Effect of sodium dodecylsulfate and benzotriazole on the interfacial behavior of Cu/Cu(II), H_2SO_4. *Mater. Chem. Phys.* **2003**, *78*, 448.

(11) Free, M. L. Understanding the effect of surfactant aggregation on corrosion inhibition of mild steel in acidic medium. *Corros. Sci.* **2002**, *44*, 2865.

(12) Villamil, R. F. V.; Corio, P.; Rubim, J. C.; Agostinho, S. M. L. Sodium dodecylsulfate-benzotriazole synergistic effect as an inhibitor of processes on copper vertical bar chloridric acid interface. *J. Electroanal. Chem.* **2002**, *535*, 75.

(13) Houyi, M.; Shenhao, C.; Bingsheng, Y.; Shiyong, Z.; Xiangqian, L. Impedance spectroscopic study of corrosion inhibition of copper by surfactants in the acidic solutions. *Corros. Sci.* **2003**, *45*, 867.

(14) Tang, L.; Mu, G.; Liu, G. The effect of neutral red on the corrosion inhibition of cold rolled steel in 1.0 M hydrochloric acid. *Corros. Sci.* **2003**, *45*, 2251.

(15) Fuchs−Godec, R.; Doleček, V. A effect of sodium dodecylsulfate on the corrosion of copper in sulphuric acid media. *Colloids Surf., A* **2004**, *244*, 73.

(16) Fuchs−Godec, R. The adsorption, cmc determination and corrosion inhibition of some *N*-alkyl quaternary ammonium salts on carbon steel surface in 2 M H_2SO_4. *Colloids Surf., A* **2006**, *280*, 130.

(17) Fuchs−Godec, R. Effect of the nature of the counterions of N-alkyl quaternary ammonium salts on inhibition of the corrosion process. *Acta Chim. Slov.* **2007**, *54*, 492.

(18) Hosseini, M.; Mertens, F. L.; Arshadi, M. R. Synergism and antagonism in mild steel corrosion inhibition by sodium dodecylbenzenesulphonate and hexamethylenetetramine. *Corros. Sci.* **2003**, *45*, 1473.

(19) Keera, S. T.; Deyab, M. A. Effect of some organic surfactants on the electrochemical behaviour of carbon steel in formation water. *Colloids Surf., A* **2005**, *266*, 129.

(20) Algaber, A. S.; El-Nemma, E. M.; Saleh, M. M. Effect of octylphenol polyethylene oxide on the corrosion inhibition of steel in 0.5 M H_2SO_4. *Mater. Chem. Phys.* **2004**, *86*, 26.

(21) Migahed, M. A. Electrochemical investigation of the corrosion behaviour of mild steel in 2 M HCl solution in presence of 1-dodecyl-4-methoxy pyridinium bromide. *Mater. Chem. Phys.* **2005**, *93*, 48.

(22) Fuchs−Godec, R. Inhibitory effect of non-ionic surfactants of the TRITON-X series on the corrosion of carbon steel in sulphuric acid. *Electrochim. Acta* **2007**, *52*, 4974.

(23) Fuchs−Godec, R. Effects of surfactants and their mixtures on inhibition of the corrosion process of ferritic stainless steel. *Electrochim. Acta* **2009**, *54*, 2171.

(24) Fuchs−Godec, R.; Žerjav, G. Inhibition properties of TRITON-X-100 on ferritic stainless steel in sulphuric acid at increasing temperature. *Acta Chim. Slov.* **2009**, *56*, 78.

(25) Asefi, D.; Mahmoodi, N. M.; Arami, M. Effect of nonionic cosurfactants on corrosion inhibition effect of cationic gemini surfactant. *Colloids Surf., A* **2010**, *355*, 183.

(26) Sherif, E. M.; Park, S.-M. Effects of 2-amino-5-ethylthio-1,3,4-thiadiazole on copper corrosion as a corrosion inhibitor in aerated acidic pickling solutions. *Electrochim. Acta* **2006**, *51*, 6556.

(27) Sherif, E.-S. M. Effects of 2-amino-5-(ethylthio)-1,3,4-thiadiazole on copper corrosion as a corrosion inhibitor in 3% NaCl solutions. *Appl. Surf. Sci.* **2006**, *252*, 8615.

(28) Sherif, E. M.; Park, S.-M. 2-Amino-5-ethyl-1,3,4-thiadiazole as a corrosion inhibitor for copper in 3.0% NaCl solutions. *Corros. Sci.* **2006**, *48*, 4065.

(29) Sherif, E.-S. M.; Shamy, A. M.; Ramla, M. M.; El Nazhawy, A. O. H. 5-(Phenyl)-4H-1,2,4-triazole-3-thiol as a corrosion inhibitor for copper in 3.5% NaCl solutions. *Mater. Chem. Phys.* **2007**, *102*, 231.

(30) Vastag, Gy.; Szöcs, E.; Shaban, A.; Kálmán, E. New inhibitors for copper corrosion. *Pure Appl. Chem.* **2001**, *73*, 1861.

(31) Ma, H. Y.; Chen, S. H.; Yin, B. S.; Zhao, S. Y.; Liu, X. Q. Impedance spectroscopic study of corrosion inhibition of copper by surfactants in the acidic solutions. *Corros. Sci.* **2003**, *45*, 867.

(32) Subramanian, A.; Rathina Kumar, R.; Natesan, M.; Vasudevan, T. The performance of VPI-coated paper for temporary corrosion prevention of metals. *Anti-Corros. Methods Mater.* **2002**, *49*, 354.

(33) Abed, Y.; Kissi, M.; Hammouti, B.; Taleb, M.; Kertit, S. Comparative study of the effect of inorganic ions on the corrosion of Al 3003 and 6063 in carbonate solution. *Prog. Org. Coat.* **2004**, *50*, 144.
(34) Asan, A.; Kabasakaloğlu, M.; Işikan, M.; Kiliç, Z. Corrosion inhibition of brass in presence of terdentate ligands in chloride solution. *Corros. Sci.* **2005**, *47*, 1534.
(35) Osman, M. M. Corrosion inhibition of aluminium−brass in 3.5% NaCl solution and sea water. *Mater. Chem. Phys.* **2001**, *71*, 12.
(36) Karpagavalli, R.; Rajeswari, S. Corrosion control of brass in groundwater by interface and interphase inhibitors. *Anti-Corros. Methods Mater.* **1998**, *45*, 333.
(37) Berchmans, L. J.; Iyer, S. V.; Sivan, V. 1,2,4,5 tetrazo spiro (5,4) decane-3 thione as a corrosion inhibitor for arsenical aluminium brass in 3.5% NaCl solution. *Anti-Corros. Methods Mater.* **2001**, *48*, 376.
(38) Ashassi-Sorkhabi, H.; Ghasemi, Z.; Seifzadeh, D. The inhibition effect of some amino acids towards the corrosion of aluminum in 1 M HCl + 1 M H_2SO_4 solution. *Appl. Surf. Sci.* **2005**, *249*, 408.
(39) Khaled, K. F. Electrochemical investigation and modeling of corrosion inhibition of aluminum in molar nitric acid using some sulphur-containing amines. *Corros. Sci.* **2010**, *52*, 2905.
(40) Saliba-Silva, A.; Faria, R. N.; Baker, M. A. Improving the corrosionresistance of NdFeB magnets:an electrochemical and surface analytical study. *Surf. Coat. Technol.* **2004**, *185*, 321.
(41) de Souza, S.; Yoshikawa, D. S.; Izaltino, W. A. S.; Assis, S. L.; Costa, I. Self-assembling molecules as corrosion inhibitors for 1050 aluminum. *Surf. Coat. Technol.* **2010**, *204*, 3238.
(42) Negm, N. A.; Al Sabagh, A. M.; Migahed, M. A.; Abdel Bary, H. M.; El Din, H. M. Effectiveness of some diquaternary ammonium surfactants as corrosion inhibitors for carbon steel in 0.5 M HCl solution. *Corros. Sci.* **2010**, *52*, 2122.
(43) Ferreira, E. S.; Giacomelli, C.; Giacomelli, F. C.; Spinelli, A. Evaluation of the inhibitor effect of-ascorbic acid on the corrosion of mild steel. *Mater. Chem. Phys.* **2004**, *83*, 129.
(44) Kertit, S.; Hammouti, B. Corrosion inhibition of iron in 1M HCl by 1-phenyl-5-mercapto-1,2,3,4-tetrazole. *Appl. Surf. Sci.* **1996**, *93*, 59.
(45) Bentiss, F.; Traisnel, M.; Gengembre, L.; Lagrenée, M. A new triazole derivative as inhibitor of the acid corrosion of mild steel: electrochemical studies, weight loss determination, SEM and XPS. *Appl. Surf. Sci.* **1999**, *152*, 237.
(46) Popova, A.; Sokolova, E.; Raicheva, S.; Christov, M. AC and DC study of the temperature effect on mild steel corrosion in acid media in the presence of benzimidazole derivatives. *Corros. Sci.* **2003**, *45*, 33.
(47) Mazhar, A. A.; Arab, S. T.; Noor, E. A. Influence of N-heterocyclic compounds on the corrosion of Al−Si alloy in hydrochloric acid-Effect of pH and temperature. *Corrosion* **2002**, *58*, 192.
(48) Oguzie, E. E.; Njoku, V. O.; Enenebeaku, C. K.; Akalezi, C. O.; Obi, C. Effect of hexamethylpararosaniline chloride (crystal violet) on mild steel corrosion in acidic media. *Corros. Sci.* **2008**, *50*, 3450.
(49) Wei, Z.; Duby, P.; Somasundaran, P. Pitting inhibition of stainless steel by surfactants: an electrochemical and surface chemical approach. *J. Colloid Interface Sci.* **2003**, *259*, 97.